Vers un modèle thermo-hydrique de sol pour application urbaine : développement numérique et premières confrontations à des mesures de terrain

Towards a thermo-hydric soil model for urban applications: numerical development and first comparisons to field measurements

Ossama LAZRAK[1]*, Thomas FASQUELLE[1], Jérôme VICENTE[1], Fabrice RIGOLLET[1]

[1] Aix Marseille Univ, CNRS, IUSTI, Marseille France
*(ossama.lazrak@univ-amu.fr)

Résumé - CityVox est un modèle de microclimat urbain en cours de développement, destiné à intégrer une reconstruction géométrique LiDAR à des simulations physiques. Le sol est modélisé en résolvant séparément les équations de la chaleur et de Richards à l'aide d'un schéma implicite en différences finies, des fonctions hydrauliques de van Genuchten et des itérations de Picard. Les simulations sont comparées au modèle de référence HYDRUS1D et à des mesures de terrain sur un sol. Les résultats sont globalement cohérents et soutiennent une validation progressive avant le couplage thermo-hydrique.

Abstract - CityVox is an urban microclimate model under development designed to integrate LiDAR-based geometric reconstruction with physical simulations. The soil component is addressed by solving the heat equation and the Richards equation separately using an implicit finite-difference scheme with van Genuchten hydraulic functions and Picard iterations. Simulations are compared with the reference model HYDRUS-1D and with field measurements on a natural soil. The results are globally consistent and support the step-by-step validation of the model prior to future thermo-hydric coupling.

Nomenclature

θ	volumetric water content, m^3/m^3	T	temperature, K or °C
θ_s	saturated water content, m^3/m^3	t	time, s
θ_r	residual water content, m^3/m^3	ρ	density, $kg \cdot m^{-3}$
α_{vg}	shape parameter, m^{-1}	c	volumetric heat capacity, $J \cdot m^{-3} \cdot K^{-1}$
n	pore-size distribution parameter	k	thermal conductivity, $W \cdot m^{-1} \cdot K^{-1}$
m	scaling law parameter, /	ε	emissivity, /
K	unsaturated hydraulic conductivity, $m.s^{-1}$	σ	Stefan–Boltzmann constant, $W \cdot m^{-2} \cdot K^{-4}$
K_s	saturated hydraulic conductivity, $m.s^{-1}$	C	specific moisture capacity, m^{-1}
S_e	effective saturation, /	q_s	surface water flux density, /
h	pressure head, m		

https://doi.org/10.25855/SFT2026-039

1. Introduction

Urban microclimate modeling relies on an accurate description of surface–atmosphere exchanges, in which soil temperature and moisture play a central role. However, soil thermo-hydric processes are often oversimplified in urban-scale models [1], partly due to the difficulty of validating physically based formulations under real conditions, as illustrated for instance by frameworks such as SOLENE-Microclimat, where soil formulations are primarily designed to support surface energy balance over urban ground, and evaporation is parameterized at the surface rather than resulting from an explicitly validated subsurface hydrological model [2].

CityVox is an urban microclimate model under development that aims to integrate LiDAR-based geometric reconstruction with physically based simulations. In this context, the soil component is validated independently using a step-by-step approach, starting with one-dimensional heat and water transfer models prior to coupling with surface energy balance and atmospheric processes. The objectives of this work are to benchmark the numerical implementation against HYDRUS-1D, analyze hydraulic parameter sensitivity and inverse estimation feasibility, and compare thermal and hydraulic simulations with outdoor measurements.

2. Method

2.1. Experimental set-up

Soil temperature and volumetric water content (VWC) were monitored continuously on a natural, unmodified soil located on a university campus in Marseille. The soil is representative of the mineral base underlying many urban surfaces prior to artificial covering and provides reference data for validating one-dimensional heat and water transfer models. Measurements were performed using a 90 cm long GroPoint multi-segment probe installed vertically, instrumenting the upper 60 cm of soil and providing simultaneous temperature and VWC data at multiple depths, with nominal accuracies of ±0.5 °C and ±2%, respectively (Table 1). The probe was connected to an autonomous DELTAOHM data logger, allowing continuous outdoor measurements over more than three months.

Atmospheric forcing was obtained from nearby meteorological stations measuring air temperature, humidity, wind speed, and solar irradiance, complemented by a local Davis station to improve representativeness. No site-specific calibration of the VWC sensor was applied, as the focus is on moisture dynamics rather than absolute values; manufacturer calibration was therefore considered sufficient for this initial validation step.

Parameter	Measurements range	Accuracy
Moisture	0% to 100% of VMC	±2.0%
Temperature	-20°C to +70°C	±0.5°C

Table 1: Measurement Reliability & Operating Limits (according to manufacturer).

2.2. Numerical model

2.2.1. Water transfer model

Water transfer in the soil is described using the one-dimensional Richards equation [3], derived from mass conservation and Darcy's law, the water balance can be written as:

$$\frac{\partial \theta}{\partial h} = -\frac{\partial q}{\partial z} \quad (1)$$

where q is the vertical water flux ($m \cdot s^{-1}$), expressed using Darcy's law for variably saturated media, accounting for both moisture dependence and gravity:

$$q = K(h)\left(\frac{\partial h}{\partial z} + 1\right) \tag{2}$$

where the gravity term arises from the vertical coordinate z oriented positively downward. The mixed formulation in terms of pressure head h gives:

$$C(h)\frac{\partial h}{\partial t} = \frac{\partial}{\partial z}\left[K(h)\left(\frac{\partial h}{\partial z} + 1\right)\right] \tag{3}$$

where C(h)=∂θ/∂h is the specific moisture capacity, θ the volumetric water content, and K(h) the unsaturated hydraulic conductivity. They are described using the semi-empirical van Genuchten–Mualem model (Eqs. 4–5), which provides a realistic representation of soil water retention and conductivity as functions of pressure head [4].

$$\theta(h) = \theta_r + \frac{\theta_s - \theta_r}{[1 + (\alpha \cdot h)^n]^m} \qquad with \qquad m = 1 - \frac{1}{n} \tag{4}$$

$$K(h) = K_s \cdot S_e^l \left[1 - \left(1 - S_e^{\frac{1}{m}}\right)^m\right]^2 \tag{5}$$

where S_e is the effective saturation and $\theta_r, \theta_s, \alpha, n, K_s, l$ are soil parameters [5].

The equation is discretized using an implicit finite-difference scheme in space and time and solved with a modified Picard iteration [3] using the Tridiagonal Matrix Algorithm (TDMA), ensuring numerical stability; lateral flow is neglected and the soil is assumed vertically homogeneous.

2.2.2. Heat transfer model

Heat transfer in the soil is modelled using the one-dimensional heat conduction equation:

$$\rho \cdot c_p \frac{\partial T}{\partial t} = \frac{\partial}{\partial z}\left(k \cdot \frac{\partial T}{\partial z}\right) \tag{6}$$

where $T\ [K]$ is the soil temperature, $\rho c_p\ [J.m^{-3}K^{-1}]$ the volumetric heat capacity, and $k\ [W.m^{-1}K^{-1}]$ the thermal conductivity, assumed isotropic and constant with temperature. A measured soil temperature time series is imposed at the lower boundary ($z = 0.33$), while surface energy exchanges account for measured solar radiation Q_{SW}, longwave radiation with the sky, and convective heat transfer with the air; water fluxes, phase change, and latent heat effects are neglected.

$$-k\frac{\partial T}{\partial z}\bigg|_{z=0} = (1-\alpha)Q_{SW} + \sigma\left(\varepsilon_{sky}T_{sky}^4 - \varepsilon_{surf}T_s^4\right) + h_c(T_{air} - T_s) \tag{7}$$

The heat equation is solved using the same implicit finite difference discretization as the water model. The resulting tridiagonal system of equations is solved using the TDMA.

3. Results and discussion

3.1. Numerical results

3.1.1. Validation of the water model against Hydrus1D

HYDRUS-1D solves the same governing equation (1) and includes the van Genuchten–Mualem hydraulic functions, making it a suitable reference for benchmarking the developed solver [6]. The comparison was conducted for a simple infiltration case in a homogeneous 1 m soil column using silt parameters from the HYDRUS-1D database (Table 2).

θ_r	θ_s	α (m^{-1})	n	K_s $(m.s^{-1})$	l
0.034	0.46	1.6	1.37	6.944·10^{-7}	0.5

Table 2: Silt soil hydraulic properties parameters [5].

A constant downward surface flux of $q_s = 5 \cdot 10^{-7}\, m.s^{-1}$ was imposed, with a constant pressure head $h = -10\ m$ prescribed at the bottom boundary. The initial condition consisted of a uniform pressure head over the profile, and the simulation was run for ten days. Figure (2) presents the time evolution of VWC at three observation depths, while Figure (3) shows the corresponding vertical moisture profiles at selected times.

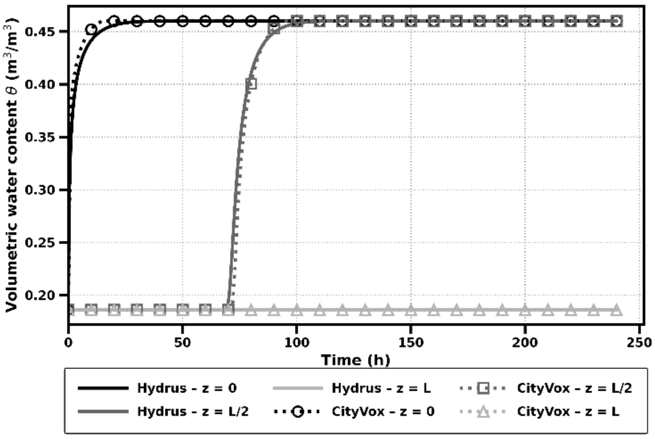

Figure 1: Time evolution of volumetric water content θ at three depths (surface, mid-depth, and bottom) simulated by Hydrus-1D and the CityVox water module.

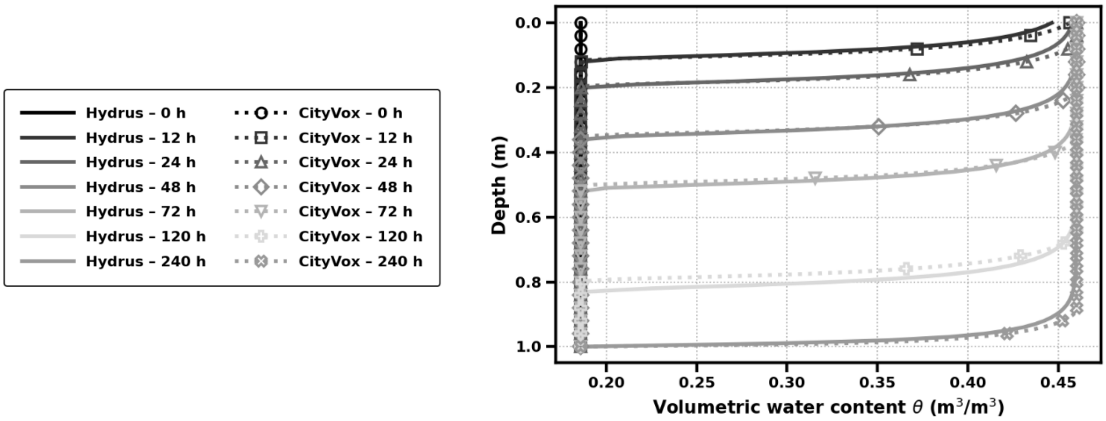

Figure 2: Vertical profiles of θ(z) simulated by Hydrus-1D and CityVox at selected times.

Both models reproduce the same infiltration dynamics and wetting front propagation, with similar timing and final moisture levels. Minor differences are observed during the transient phase at intermediate depths, with HYDRUS-1D exhibiting a slightly smoother moisture evolution. Overall, the comparison confirms the correct implementation of the Richards equation and the van Genuchten–Mualem hydraulic formulation in the developed solver.

3.1.2. Water model sensitivity analysis

A local sensitivity analysis was performed to evaluate how the Richards solver responds to variations in soil hydraulic parameters. This analysis used constant flux infiltration. Starting from a reference parameter set, each parameter was independently disturbed by ±1% around a reference silt parameter set (Table 1), and sensitivities were computed using a central finite-difference approximation and normalized to obtain dimensionless coefficients $S_{pj}(t)$.

$$S_{pj}(t) = \frac{p_j}{\theta(t)} \frac{\partial\theta(t)}{\partial p_j} \tag{8}$$

Six van Genuchten-Mualem parameters were considered. Figure (4) presents their time-averaged sensitivity coefficients $\overline{S_{pj}}$, showing that sensitivity magnitude varies across parameters and over the simulation period (10 days).

$$\overline{S_{pj}} = \frac{1}{N_t}\sum_{i=1}^{N_t}\left|S_{pj}(t)\right| \tag{9}$$

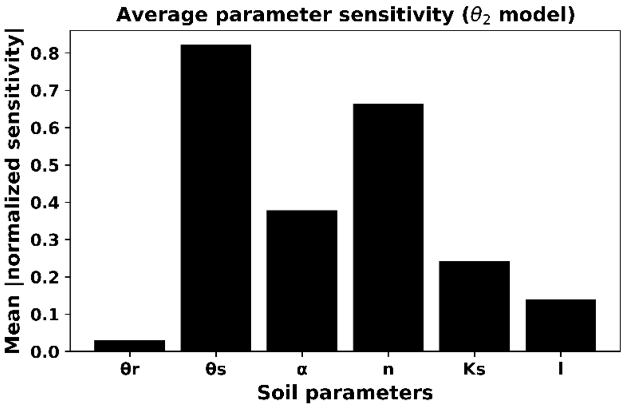

Figure 3: The average sensitivity.

This sensitivity analysis was conducted to identify which parameters have a measurable influence on the model outputs. The results show that the model response is primarily sensitive to the saturated water content θ_s and to the shape parameters n and α. These findings justify focusing the inverse parameter estimation on θ_s, n, and α.

3.1.3. Inverse parameter estimation

Parameter estimation was performed using measured VWC time series as boundary conditions, with the measured $\theta_1(t)$ and $\theta_3(t)$ imposed as Dirichlet conditions at the upper and lower boundaries, respectively, and the Richards model used to simulate the intermediate VWC: $\theta_2(t)$. The calibration problem is formulated as the minimization of the sum of squared errors between simulated and measured $\theta_2(t)$, with the objective function defined as:

$$J(p) = \sum_t \left[\theta_{2,model}(t;p) - \theta_{2,meas}(t)\right]^2 \tag{6}$$

where the parameter vector $p = (n, \alpha)$. Despite its high sensitivity, θ_s was fixed, together with θ_r, to physically plausible values consistent with the observed VWC range, while the remaining parameters are kept constant to limit non-uniqueness in the inverse problem. Minimization is performed using a Levenberg–Marquardt algorithm, where the Jacobian matrix is approximated by central finite differences, and the resulting parameter estimates are presented in the VWC model calibration section table (3).

3.2. Comparison with results from the experimental set-up

3.2.1. Volumetric water content

Measured and simulated VWC at the intermediate depth were compared using a calibration–validation approach. The comparison focuses on the model's ability to reproduce the time evolution of soil moisture under measured boundary forcing over a one-dimensional soil column of thickness $L = 0.3$ m, discretized into $n = 201$ uniform vertical nodes.

3.2.1.1. Calibration

Calibration was first performed over a drying period. Measured water content was imposed at the upper and lower boundaries (θ_1 & θ_3), and the parameters $\boldsymbol{n}$ and $\boldsymbol{\alpha}$ were estimated using Levenberg–Marquardt. The optimization was initialized from physically plausible values and converged in fewer than 15 iterations.

θ_r	θ_s	α	n	K_s	l
0.001	0.49	**1.699**	**3.01**	8.10^{-6}	0.5

Table 3: estimated soil properties parameters.

Figure (5) compares measured and simulated VWC during the calibration period, showing that the model reproduces the overall drying trend and temporal evolution, with only minor short-term discrepancies and no systematic drift.

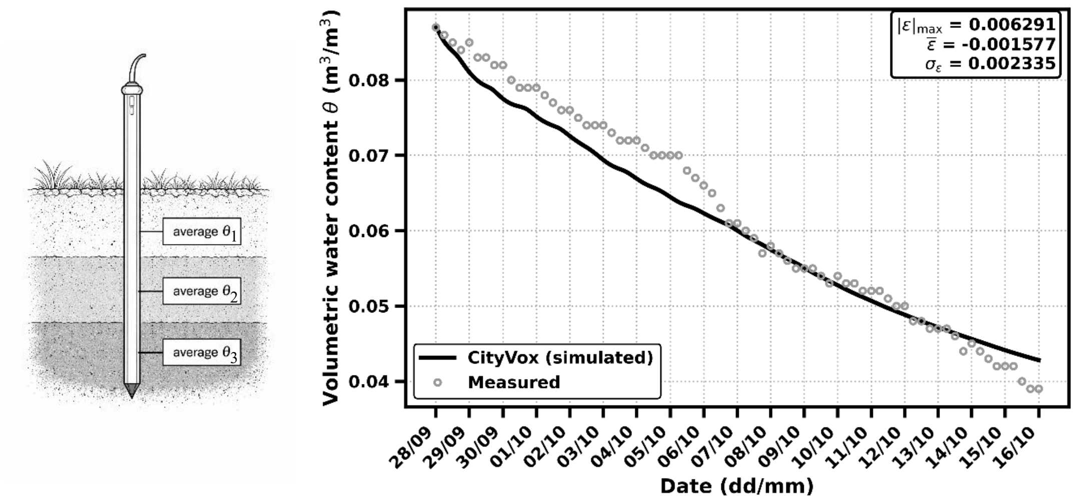

Figure 4: Calibration of the Richards-based model against θ_2, a measured 15 cm averaged VWC.

3.2.1.2. Comparison modeled vs measured VWC

The calibrated parameters were applied unchanged to an independent validation period, and Figure (6) compares the measured and simulated VWC.

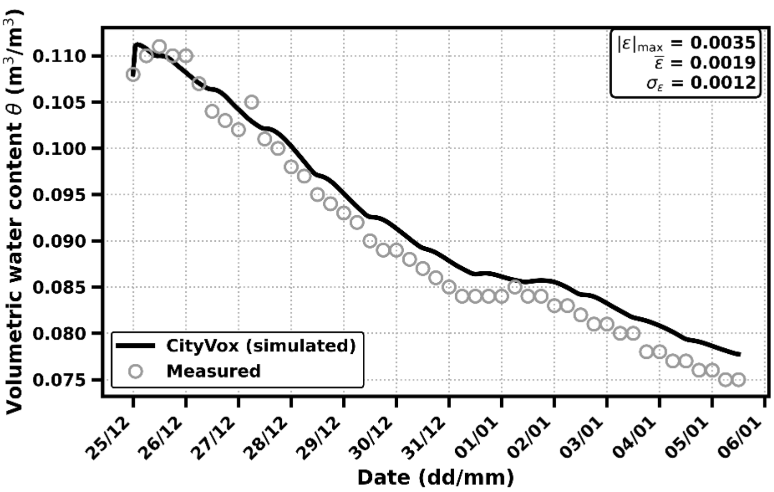

Figure 5: Comparison between measured and simulated VWC (θ_2) during the validation period.

The model preserves the general moisture dynamics, including the long-term drying behavior. The agreement is characterized by low absolute errors (mean ≈ $2{\cdot}10^{-3}$ $m^3{\cdot}m^{-3}$), comparable to the measurement uncertainty, while larger deviations occur during short-term fluctuations, likely linked to near-surface processes and the simplified 1D soil representation.

3.2.2. Temperature profiles

Comparison between measured and simulated soil temperature time series at the instrumented depths of the soil can be found on Figure (7). The thermal model was driven by measured atmospheric forcing and measured boundary conditions, without calibration of thermal parameters, which are assumed homogeneous and constant as listed in Table 4.

The model reproduces the main thermal dynamics with depth-dependent accuracy. Quantitatively, the maximum absolute error decreases from about 4.1 °C at 3 cm depth to 1 °C–1.3 °C below 13 cm, with mean errors remaining below 0.3 °C at all depths. The larger discrepancies near the surface are attributed to the absence of measured net radiation forcing, as surface layers are more sensitive to radiative exchanges, while deeper layers are dominated by conductive heat transfer. In addition, the convective heat transfer coefficient was prescribed as a constant value ($h_c = 10\, W.m^{-2}.K^{-1}$) representative of typical outdoor conditions, although it varies with wind speed.

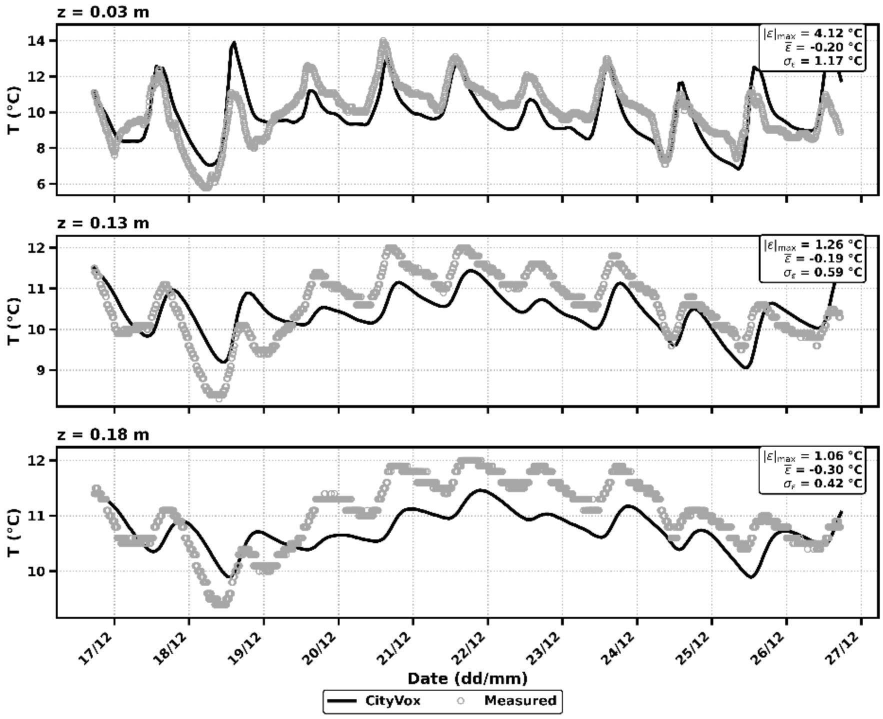

Figure 6: Comparison between measured and simulated soil temperature with error metrics.

Zone	Thickness (m)	k (W.m^{-1}.K^{-1})	ρ (kg.m^{-3})	c_p (J.kg^{-1}.K^{-1})	Cell Count
1	0.04	0.8333	1350	2400	10
2	0.12	0.8333	1350	2400	26
3	0.16	0.8333	1350	2400	16
4	0.01	0.8333	1350	2400	2

Table 4: Domain and Mesh Overview.

3.3. Discussion

The model reproduces the dominant temporal dynamics of soil moisture and temperature under real atmospheric forcing; however, the validation is intentionally constrained and non-predictive. Moisture validation relies on prescribed volumetric water content at both boundaries

(Dirichlet–Dirichlet), which isolates internal redistribution governed by the Richards equation but suppresses uncertainties related to infiltration, evaporation, and drainage, thereby limiting physical realism and the identifiability of hydraulic parameters. Consequently, estimated parameter values should not be interpreted as physical soil properties, as they are primarily influenced by the adopted boundary conditions and limited observational constraints. Remaining VWC discrepancies are consistent with unresolved soil heterogeneity and the absence of site-specific sensor calibration, restricting interpretation to temporal dynamics rather than absolute values.

Temperature simulations exhibit better agreement than moisture simulations due to the diffusive nature of heat transfer and its lower sensitivity to heterogeneity. Near-surface temperature errors reflect a limitation of the thermal forcing, as net radiation was not measured and longwave exchange was parameterized, with air temperature and incoming shortwave radiation as the only in-situ forcings.

4. Conclusion and perspectives

This study presented the numerical development and first-stage validation of a one-dimensional soil thermo-hydric model intended for integration into the CityVox framework. Benchmarking against HYDRUS-1D confirmed the numerical correctness of the Richards solver, while experimental comparisons demonstrated the model's ability to reproduce the dominant temporal behavior of soil moisture and temperature under constrained boundary conditions.

The scope of this validation is intentionally limited by simplifying assumptions, including homogeneous soil properties, prescribed moisture boundaries, simplified thermal forcing, and the absence of evaporation and thermo-hydric coupling. These choices were made to reduce external uncertainties and to assess internal model consistency prior to introducing additional physical complexity. Future work will focus on relaxing these constraints through coupled thermo-hydric formulations, flux-based boundary conditions, inverse estimation of soil thermal properties, and improved surface energy balance forcing, which are necessary steps toward predictive soil–atmosphere interactions in urban contexts.

References

[1] H. Vereecken *et al.*, "Modeling Soil Processes: Review, Key Challenges, and New Perspectives," *Vadose Zone J.*, vol. 15, no. 5, pp. 1–57, May 2016, doi: 10.2136/vzj2015.09.0131.

[2] M.-H. Azam, B. Morille, J. Bernard, M. Musy, and F. Rodriguez, "A new urban soil model for SOLENE-microclimat: Review, sensitivity analysis and validation on a car park," *Urban Clim.*, vol. 24, pp. 728–746, Jun. 2018, doi: 10.1016/j.uclim.2017.08.010.

[3] M. W. Farthing and F. L. Ogden, "Numerical Solution of Richards' Equation: A Review of Advances and Challenges," *Soil Sci. Soc. Am. J.*, vol. 81, no. 6, pp. 1257–1269, Nov. 2017, doi: 10.2136/sssaj2017.02.0058.

[4] M. Th. Van Genuchten, "A Closed-form Equation for Predicting the Hydraulic Conductivity of Unsaturated Soils," *Soil Sci. Soc. Am. J.*, vol. 44, no. 5, pp. 892–898, Sep. 1980, doi: 10.2136/sssaj1980.03615995004400050002x.

[5] Y.-B. Li, Y. Liu, W.-B. Nie, and X.-Y. Ma, "Inverse Modeling of Soil Hydraulic Parameters Based on a Hybrid of Vector-Evaluated Genetic Algorithm and Particle Swarm Optimization," *Water*, vol. 10, no. 1, p. 84, Jan. 2018, doi: 10.3390/w10010084.

[6] J. Å imunek, M. Th. Van Genuchten, and M. Å ejna, "HYDRUS: Model Use, Calibration, and Validation," *Trans. ASABE*, vol. 55, no. 4, pp. 1263–1276, 2012, doi: 10.13031/2013.42239.

Acknowledgements

The authors gratefully acknowledge the financial support of MITI CNRS (Mission pour les Initiatives Transverses et Interdisciplinaires), as well as the support of the IUSTI laboratory.